Crystallization Behavior of Elastomeric Block Copolymers: Thermoplastic Polyurethane and Polyether-*block*-Amide

Asli Begenir, Stephen Michielsen, Behnam Pourdeyhimi

Nonwovens Cooperative Research Center, North Carolina State University, Raleigh, North Carolina 27695-8301

Received 27 March 2008; accepted 21 July 2008
DOI 10.1002/app.29082
Published online 22 October 2008 in Wiley InterScience (www.interscience.wiley.com).

ABSTRACT: The isothermal crystallization kinetics of melt-blown webs produced from a series of elastomeric block copolymers was studied through differential scanning calorimetry (DSC). Three hardness grades were selected for a polyester and a polyether Elastollan® thermoplastic polyurethane and Pebax® polyether-*block*-amide copolymers. The Avrami crystallization kinetics parameters, *k* and *n*, were derived from two different methods: (1) traditional Avrami model and (2) derivative of the Avrami model proposed by Kurajica et al. (Croat Chem Acta 2002, 75, 693). The kinetic parameters from both models were consistent and showed good correlation. For all polymer types and hardness grades, crystallization kinetics were interpreted with the derivative model (Kurijica et al.) since it could be directly fitted to untransformed DSC isothermal crystallization data, and thus reduces the errors involved in Avrami analysis. The values of the Avrami exponent, *n* ranged between 2.59 and 3.41, indicating similar nucleation and growth mechanisms. These *n* values and morphological observations indicate that crystallization occurs in these copolymers in three dimensions from pre-existing nuclei and the crystals grow under isothermal conditions. This suggests that, in these elastomeric copolymers, crystallization of the hard segments drives microphase separation into crystalline and amorphous regions rather than formation of hard and soft domains. © 2008 Wiley Periodicals, Inc. J Appl Polym Sci 111: 1246–1256, 2009

Key words: polyurethane; crystallization; Avrami; thermoplastic elastomer

INTRODUCTION

Thermoplastic polyurethane (TPU) and polyether-*block*-amide (PEBA) elastomers are semicrystalline block copolymers that consist of two phases: hard and soft segments. These polymers exhibit elastomeric properties at room temperature, but can be processed like plastics at high temperature. Although the amorphous soft segments provide rubber-like properties, hard segments crystallize, thereby forming a thermally reversible network structure responsible for the mechanical properties, i.e., the crystallized hard segments behave as physical crosslinks. In typical TPU elastomers, hard segments are created by the reaction of a diisocyanate with low-molecular weight diols, yielding hard segments with urethane groups. Typically, soft segments are polyether or polyester polyols. In PEBA elastomers, hard polyamide segments are connected to soft segments through ester groups. The PEBA series studied here consists of polyamide 12 hard segments and poly(tetramethylene oxide)glycol (PTMO) soft segments.[1–3]

It is well established that the morphology of semicrystalline block copolymers depends strongly on the interaction between two self-organizing mechanisms: crystallization of hard segments and microphase separation to form domains due to incompatibility and immiscibility of hard and soft segments. In TPU and PEBA block copolymers, crystallization occurs through association of hard segments via hydrogen bonding between urethane and amide groups, respectively.[4–6] Domain formation and microphase separation in block copolymers depend on how crystallization proceeds. Microphase separation may precede crystallization from disordered melt, or crystallization may drive microphase separation from disordered melt when block incompatibility is small. Depending on the strength of segregation, degree of cooling, glass-transition temperature of the amorphous segments, and competition between crystallization and diffusion rates, crystallization may proceed within the preexisting domains or it may destroy existing microphase-separated domains.[4,7] When block copolymers crystallize from a single-phase melt, their crystallization behavior is similar to homopolymers. In this case, crystals can grow freely and aggregate to form macroscopic structures such as spherulites since there are no

Correspondence to: S. Michielsen (smichie@ncsu.edu).
Contract grant sponsors: Hanes Brands Inc. (HBI), Nonwovens Cooperative Research Center (NCRC).

existing domains to restrict the crystal growth. However, in strongly phase-separated melts, crystal growth is restricted in one direction since crystallization is confined to microdomains. This leads to nanoscale crystal structures. These morphological differences affect the crystallization kinetics. When crystallization drives microphase separation either from homogeneous melt or by destroying an existing domain structure, the Avrami model describes the characteristic sigmoidal crystallization kinetics at early stages of isothermal crystallization. For crystallization isolated to domains, crystallization will follow first-order kinetics along with very small Avrami n values ($n < 1$).[7–14]

Many earlier studies investigating the morphology of block copolymers consisting of crystalline hard and flexible amorphous soft segments have been reported. In a series of morphological studies of ether–ester copolymers, Wegner et al.[14–17] observed formation of spherulitic crystals in the amorphous matrix, which was similar to the crystallization of homopolymers rather than microphase separation as observed in block copolymers. Ho et al.[18] suggested spherulitic crystallization of hard segments with no macrophase separation in ether–ester block copolymers. Seymour et al.[19] and Xu et al.[20] proposed a model of spherulitic crystallization for ester–urethane copolymers, in which microphase separation occurs only into crystalline and amorphous regions. In these models, incompatibility of hard and soft segments drives association and crystallization of hard segments rather than microphase separation into hard and soft domains. In a study of nanophase-separated Pebax 3533 and Pellethane TPU 70A with AFM, McLean and Sauer[21] observed larger crystals in PEBA than in TPU 70A. They described crystallization in PEBA as crystallization-driven phase separation, whereas in TPU crystallization was restricted to hard domains which had already phase separated.[22]

The polymers used in this study were processed via melt-blowing before measuring the crystallization kinetics. Melt-blowing is a unique nonwoven process, in which the molten polymer is extruded into high-velocity convergent air streams that stretch the polymer melt rapidly into very fine fibers. These fine fibers are then collected on a moving belt to produce self-bonding web structures. Because the polymer melt is attenuated by the air streams until reaching the air velocity or reaching the collector, the resultant fiber properties and fiber formation process depend strongly on the interaction between the processing conditions and polymer characteristics. The critical processing conditions that determine the degree of attenuation and solidification attained when the fiber interacts with the others already on the collector are mainly the air velocity, die-to-collector distance (DCD), polymer extrusion temperature, and air temperatures. As discussed earlier, the crystallization behavior of elastomeric copolymers is complex and controls the polymer properties through the morphology established during processing and solidification of these polymers. Thus, to optimize the melt-blowing process and obtain webs with better properties, it is critical to understand the correlation between the crystallization behavior of TPU and PEBA elastomers and the processing conditions, which in turn governs the web properties. Despite the fact that thermoplastic elastomers including these copolymers have found use in a variety of nonwoven applications, the literature describing their processing and use is limited to the patent literature.[23–28] Therefore, we aim to examine the relationship between the polymer material, processing conditions, and web properties in melt-blowing TPU and PEBA elastomeric copolymers. Here, we investigate the crystallization behavior of TPU and PEBA elastomers to understand the effect of polymer crystallization on melt-blowing process conditions and web properties, which will be reported in a future study.[29]

A variety of models have been developed to describe the crystallization kinetics of semicrystalline polymers under isothermal quiescent conditions.[30,31] Among these, the Avrami model has been the most commonly used to describe the kinetics of the primary crystallization stage of isothermal crystallization, which includes primary nucleation and growth of the crystal units until their impingement, followed by the secondary crystallization stage. At a given crystallization temperature, the degree of phase transformation, i.e., relative crystallinity, $X(t - t_0)$, is related to time t by the Avrami equation[32] as follows:

$$X(t - t_0) = \frac{Xc_t}{Xc_\infty} = 1 - \exp(-k(t - t_0)^n) \qquad (1)$$

where Xc_t and Xc_∞ are the amount of crystallinity at time t and at infinite time, respectively. k is the crystallization rate constant; n is the Avrami exponent; and t_0 is the time at the onset of crystallization. If one assumes that the relative degree of crystallinity increases with crystallization time, eq. (1) can be used to analyze isothermal crystallization. The crystallization rate constant, k, is a function of nucleation and growth rates, and it depends on polymer properties and temperature. The Avrami exponent, n provides information on the number of dimensions in which growth takes place (growth geometry) and on the nucleation process. According to the original assumptions of the theory, the Avrami exponent, n, ranges between the positive integers 1 and 4.[32–34]

TABLE I
Melt-Blowing Process Conditions

Sample ID			Die temp. (°C)	Air temp. (°C)	Polymer mass flow rate (ghm[a])
Ether TPU	Elastollan® C78A15	T80	233	222	0.50
	Elastollan® C85A10	T90	251	238	0.50
	Elastollan® C95A10	T98	261	249	0.50
Ester TPU	Elastollan® 1180A10	S78	253	234	0.50
	Elastollan® WY5352D-1	S95	262	261	0.50
PEBA	Pebax® 2533	P25	287	258	0.24
	Pebax® 3533	P35	305	267	0.24
	Pebax® 5533	P55	312	274	0.24

[a] ghm, grams per hole per minute.

The Avrami kinetic parameters are usually determined by taking double logarithm of eq. (1):

$$\log[-\ln(1 - X(t - t_0))] = n \log(t - t_0) + \log k \quad (2)$$

The rate constant, k, and Avrami exponent, n, are obtained by plotting the $\log[-\ln(1 - X(t - t_0))]$ against the $\log(t - t_0)$. The value of y-intercept gives $\log(k)$ while n is just the slope of the least-square line.[35]

Even though the traditional Avrami method is commonly accepted for the analysis of isothermal crystallization kinetics of polymers, it has well-known shortcomings. The Avrami equation is only valid for crystallization levels where no impingement of crystal units occurs, i.e., at short crystallization times. Because the crystallization onset, t_0, is typically determined visually on the DSC isothermal crystallization exotherm, the calculation of the relative crystallinity, $X(t - t_0)$ by integrating the DSC data inherently involves errors. In addition, the double logarithmic form of the Avrami plot may result in superficially good fits for experimental data, and thus the derived kinetic parameters may not give a true representation of the crystallization process.[18,34] Although this does not mean that the derived Avrami parameters are invalid, the evaluation of the crystallization kinetics based only on the Avrami analysis may be misleading. Among many studies attempting to improve the Avrami analysis, Kurajica et al.[31] proposed a different approach for analysis of isothermal crystallization DSC data. They took the derivative of the Avrami equation and fit the untransformed DSC data directly to this function. In their equation, they replaced k of the Avrami equation by k^n. Thus, they represented the heat flow dq/dt measured by DSC as follows:

$$\frac{dq}{dt} = \Delta H \frac{d\alpha}{dt} = \Delta H n k^n (t - t_0)^{n-1} \exp(-k^n (t - t_0)^n) \quad (3)$$

where ΔH is the enthalpy of crystallization and $d\alpha/dt$ is the change in the amount of crystalline material with time. One advantage of this approach is that dq/dt is obtained directly from the DSC data while the traditional Avrami analysis requires transformation of the DSC data from differential to integral form, which makes this traditional method very sensitive to errors. It is also worth noting that k in the Kurajica analysis has units of 1/time while in the traditional Avrami analysis, k has units of $1/\text{time}^n$.

We report the analysis of the isothermal crystallization kinetics of polyether- and polyester-based TPU and PTMO-based poly(ether-*block*-amide) (PEBA) elastomers using both the traditional Avrami analysis and the analysis of Kurajica et al.[31] In both polyether and polyester TPU elastomers, the hard segment is 4,4′-diphenylmethane diisocyanate (MDI) and 1,4-butanediol (BDO), whereas that of PEBA is polyamide 12.

EXPERIMENTAL

Melt-blown webs were produced on the North Carolina State University Nonwoven Cooperative Research Center's melt-blowing line from thoroughly dried (1) BASF Elastollan® Ether TPU series (Shore A): 1180A10, 1190A16, and WY5352D-1; (2) BASF Elastollan® Ester TPU series (Shore A): C78A15 and C95A10; and (3) Arkema Pebax® series (Shore D): 2533, 3533, 5533. Within Table I, and throughout this manuscript, ester and ether TPUs are denoted as *Sxx* and *Txx*, respectively, where xx represents Shore A hardness. Likewise, the PEBAs are referred to as *Pxx*, where xx represents Shore D hardness. These elastomers were chosen to span similar hardness ranges across all of the materials studied.

The processing conditions in melt-blowing TPU and PEBA elastomers are shown in Table I. Melt-blown webs analyzed in this study were produced at a DCD of 0.14 m. The DCD and polymer mass flow rates used are representative of commercial melt-blowing DCDs and rates. The polymer extrusion or die temperatures were adjusted for each polymer type and hardness grade to maintain the melt viscosity and die pressures in the acceptable range for an efficient melt-blowing process. The

TABLE II
DSC Crystallization Temperatures and Test Conditions

Sample ID		T_m (°C)	Crystallization T_{onset} (°C)	Crystallization T_{peak} (°C)	DSC isothermal crystallization	
					Melt temp. (°C)	Temp. range (°C)
Ether TPU	T80	146.5	79.1	71.2	195	89–93.5
	T90	165	106.2	99.3	210	110–120
	T98	183.3	118.4	112.9	225	130–146
Ester TPU	S78	158.1	81.0	71.8	215	88–93.5
	S95	196	113.2	107.7	225	124–134
PEBA	P25	135	90.1	81.6	180	84–92
	P35	142	98.6	91.1	180	96–110
	P55	161	133.8	126.8	200	138–143

resulting webs were used to determine the crystallization kinetics.

A Perkin–Elmer Diamond differential scanning calorimeter (DSC) was used to detect the thermal transitions and follow the heat flow from the web samples during isothermal crystallization from the melt. The DSC equipped with internal liquid nitrogen cooling unit reliably provided a cooling rate up to 50°C min^{-1}. At higher cooling rates, it was observed that the collected data was unreliable due to the initial instability of the DSC program versus sample temperature. Temperature calibration was performed using an indium standard ($T_m = 156.6$°C and $\Delta H = 28.5$ J g^{-1}). All DSC scans were carried out under nitrogen atmosphere, and each sample was used only once to reduce degradation. Web samples of 3–5 mg were placed in open DSC pans, vacuum-dried at 60°C for 3 h, and kept in desiccators until just before loading into the DSC.[18] To observe the crystallization exotherm and determine the onset of crystallization, web samples were first heated to temperatures 40–50°C above their peak melting temperature at 20°C min^{-1}, maintained at this temperature for 3 min to ensure complete melting, and then were cooled to 25°C at 10°C min^{-1}.[36]

To determine the rate of crystallization during isothermal crystallization, it is desirable to have crystallization times of a few minutes so that the DSC can acquire accurate data. To reduce the crystallization rate, the initial isothermal crystallization temperature was chosen by adding 5–10°C to the observed onset of crystallization temperature as seen in Table II. On subsequent isothermal crystallization runs, the isothermal temperature was increased or lowered, depending on the rate observed in the initial run. Isothermal crystallization kinetics from the melt was determined as follows. Melt-blown web samples were melted at temperatures 40–50°C above their peak melting temperature at heating rates of 20°C min^{-1}, held there for 3 min, and then cooled at 50°C min^{-1} to the desired isothermal crystallization temperature, T_c, and maintained at that temperature for 10 min until crystallization was complete. The heat flow generated as a function of time during the isothermal crystallization was recorded and analyzed to obtain relative degree of crystallinity, $X(t - t_0)$:

$$X(t - t_0) = \left(\frac{A_t}{A_\infty}\right) \quad (4)$$

where t_0 is the time at which the web sample attains stable isothermal conditions, which is assumed to correspond to the crystallization onset. A_t is the cumulative area under the exotherm from time t_0 to time t and A_∞ is the total area of the crystallization exotherm at long times.

The morphology of the melt-blown webs was observed using Metaltek Instruments Carl Zeiss optical polarizing microscope with a Mettler model FP82HT hot stage and a Diagnostic Measurements, 0.6×, HRP060-CMT camera. Meltblown web samples produced from P55, T98, and S95 were sandwiched between two microscope cover glasses, melted at 200–225°C for 3 min and then rapidly cooled to the crystallization temperature at a rate of 10°C min^{-1}. Morphology development was recorded during crystallization.

RESULTS AND DISCUSSION

Figure 1 shows a typical DSC crystallization exotherm for isothermal crystallization of the melt-blown web, T98 at $T_c = 130$°C after complete melting at 225°C for 3 min. Crystallization is assumed to begin at Point A where $t_0 = 0.778$ min, which is preceded by a short-time period during which the temperature of the web sample reached isothermal crystallization conditions and crystallization begins. The exothermic heat flow increases until reaching a maximum at Point B.[37] Beyond the maximum heat flow, crystallization slows significantly, and no noticeable change in the heat flow is detected after Point C. As expected, melting and crystallization peaks as well as onset of the crystallization shift to higher temperatures with increasing amount of crystallizable component, i.e., increasing Shore hardness. Thus, the crystallization temperature, T_c, follows the

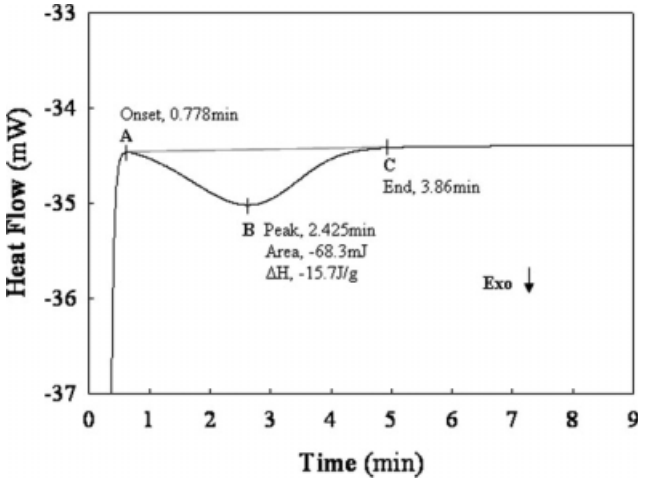

Figure 1 Isothermal crystallization of T98 melt-blown web at $T_c = 130°C$.

order of P55 > P35 > P25 for PEBA, S95 > S78 for ester TPU, and T98 > T90 > T80 for ether TPU.

The rate of heat flow during isothermal crystallization depends strongly on the kinetics of the crystallization process, which is very sensitive to crystallization temperature. This is illustrated in Figure 2, where crystallization exotherms of web T90 at several crystallization temperatures are plotted. It is clearly observed that at higher crystallization temperatures, the crystallization maxima shift to longer times and become flatter. This means that the time to reach the ultimate degree of crystallinity becomes longer and the crystallization rates decrease due to the decrease in the degree of cooling ($T_{\text{melting point}} - T_{\text{crystallization}}$). The crystallization exotherms of the other polymers studied are not shown here since all exhibited similar temperature dependency.

Figure 3 shows the development of relative crystallinity $X(t - t_0)$ with crystallization time for PEBA series. It can be seen that all exotherms exhibit characteristic sigmoidal behavior and the curves shift to longer times with increasing crystallization temperatures. The relative crystallinity versus crystallization time plots of ether and ester TPU systems are not shown here since all exhibit similar sigmoidal dependence.

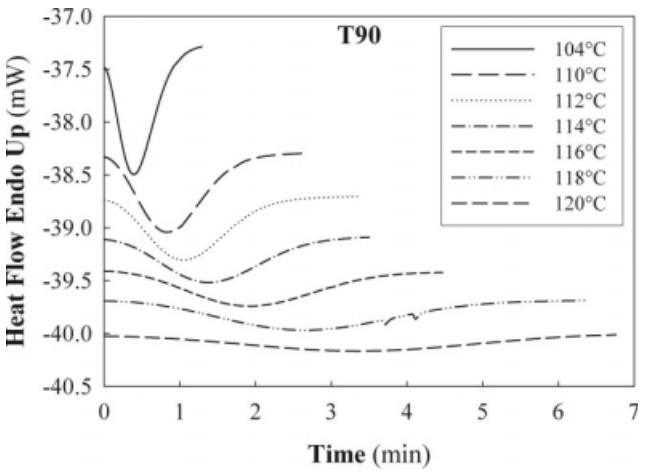

Figure 2 Isothermal crystallization of T90 melt-blown web at varying T_c.

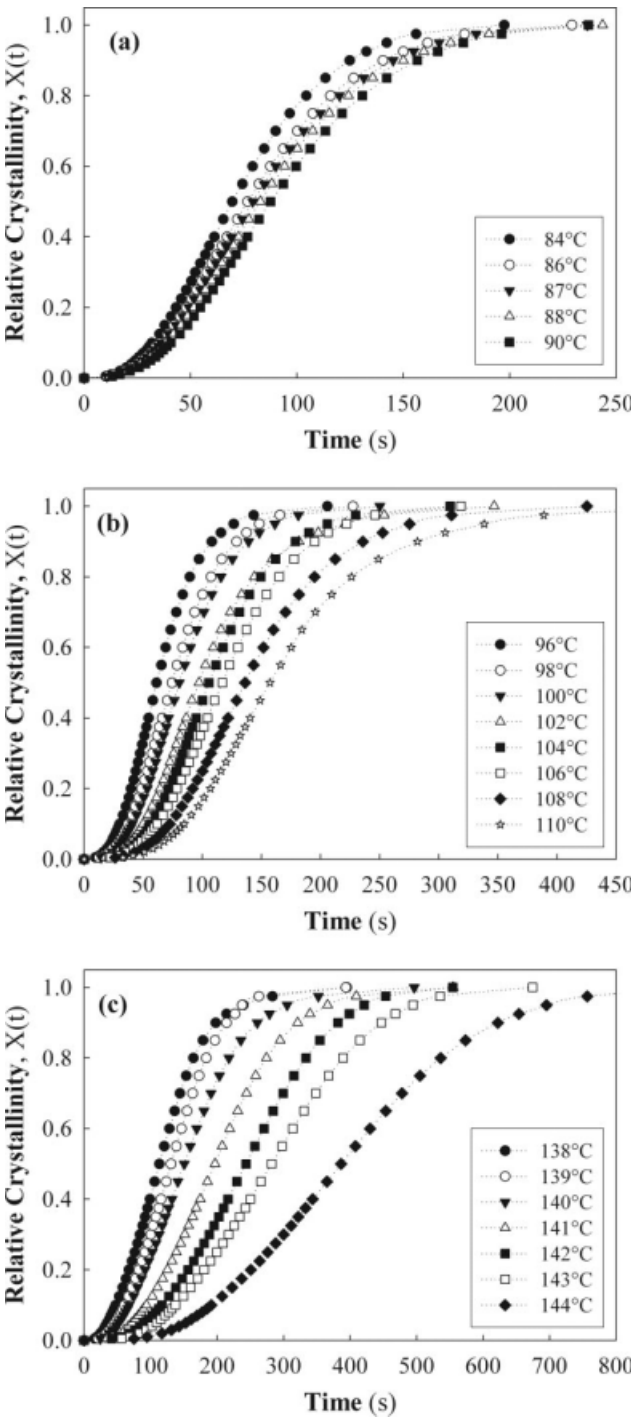

Figure 3 Relative crystallinity $X(t - t_0)$ versus crystallization time for (a) P25, (b) P35, and (c) P55.

The double logarithmic Avrami plots of $\log[-\ln(1 - X(t - t_0))]$ versus $\log(t - t_0)$ are shown in Figure 4. As observed from the plots, experimental DSC data

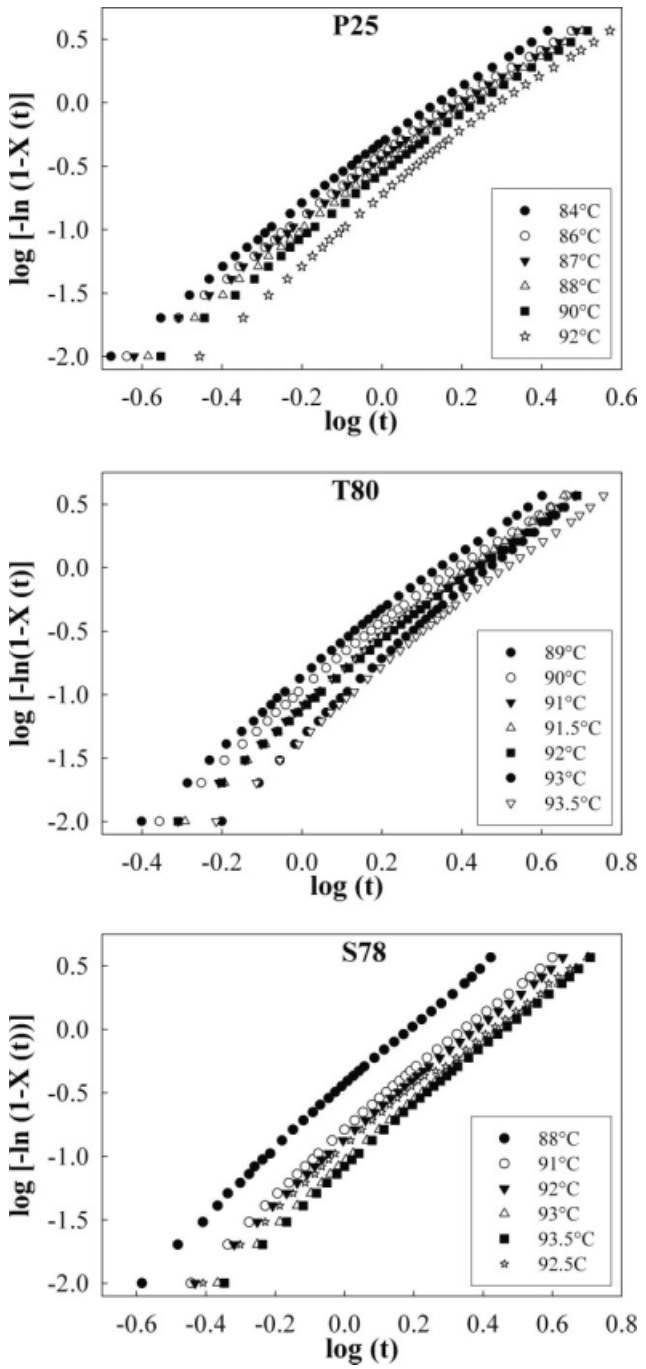

Figure 4 Avrami double logarithm plots from dried samples of P25, T80, and S78.

fit the Avrami model only for the initial portion of the crystallization process, beyond which deviations from the model are observed as changes in the slope. This is in agreement with the literature suggesting that the Avrami model is valid only for the early stages of the crystallization process. Therefore, to obtain the Avrami kinetic parameters, k and n, the experimental data at low transformations of the crystallization are used, corresponding to around $X_c < 30\%$ for soft and medium grades and <10% for the hardest grades.[34,38]

The values of the crystallization kinetics parameters determined from the DSC heat flow data using traditional Avrami analysis in eq. (2) are plotted against those derived from the Kurajica model in eq. (3) in Figure 5. A linear correlation between the n-parameters [Fig. 5(a)] obtained from both models is observed indicating that both methods give similar values. However, n obtained from the Avrami fit tends to be larger than that obtained from the Kurajica model. In Figure 5(b), the Avrami $k^{1/n}$ value is plotted against the k value from the Kurajica model. This approach accommodates the different definitions used for k in eqs. (1) and (3). There is a linear dependence of the value of k from the Kurajica model with the value of $k^{1/n}$ derived from the Avrami model. However, although there is a similar correlation for P55, the slope is quite different from the other polymers [see Fig. 5(b)]. Since the Kurajica model is less sensitive to errors, we use Kurajica's approach in the remainder of this study.

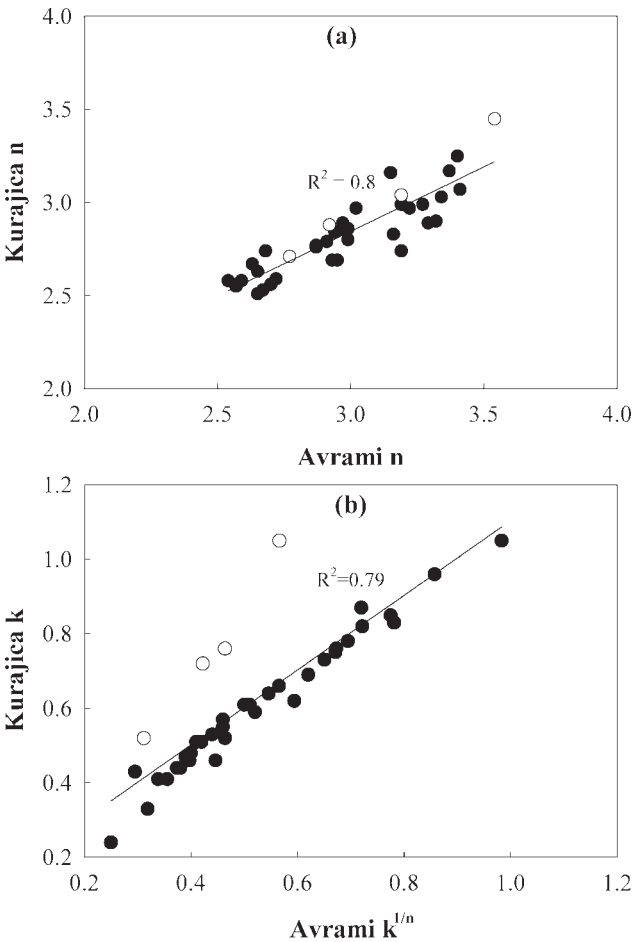

Figure 5 Comparison of the kinetic parameters derived from the Avrami model in eq. (2) and the Kurajica model in eq. (3). (a) Avrami exponent and (b) Kurajica and Avrami crystallization rates k and $k^{1/n}$, respectively. Hollow symbols represent P55.

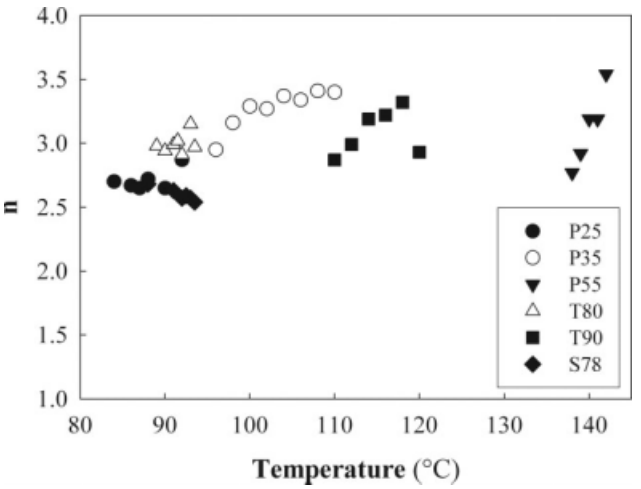

Figure 6 Avrami exponent n as a function of crystallization temperature as obtained from the Kurajica model.

Figure 6 shows the Avrami exponent, n, from eq. (3) plotted as a function of polymer type as well as isothermal crystallization temperatures. For a single polymer type, n has a weak dependence on temperature except for P55. On the other hand, k has a strong dependence on temperature (Fig. 7). As expected, k decreases with increasing crystallization temperatures, regardless of the polymer type and hardness. Because n values of nearly 3 are relatively independent of the isothermal crystallization temperatures, the mechanism of nucleation and crystal growth do not change with increasing crystallization temperatures, at least within the temperature ranges studied. The decrease in the crystallization rate is therefore due to the decrease in the rate of nucleation and crystal growth with increasing crystallization temperatures. This is expected since the energy barrier for nucleation will increase as the crystallization temperatures approach melting temperatures.[18,39,40] The values of k and n obtained from Kurajica's model are shown in Table III. Analysis of the secondary crystallization is not considered within this text because the purpose of this research is to understand the effect of crystallization kinetics in melt-blowing process where polymer melt reaches the collector within time scales significantly shorter than the onset of secondary crystallization.[29] As seen in Table III, for all studied webs, noninteger n values were obtained, contradictory to the theoretical expectations of integer values based on the original Avrami assumptions. Earlier studies interpreted noninteger n values due to simplified assumptions in the original Avrami equation, which may not apply to all polymers under all crystallization conditions,[39] the complex nature of crystallization,[33] mixed nucleation and/or crystal growth modes,[35] variations in crystal growth dimension,[41] variation in nucleation and/or crystal growth rates during crystallization,[42] development of similar crystal growth structures from different types of nuclei,[34] and simultaneous occurrence of two- and three-dimensional crystal growth.[38] As suggested by Cho et al.,[42] noninteger n values will be considered as representative of the nearest integer. Based on the characteristic sigmoidal crystallization behavior observed in Figure 3 along with n values of around 3, the crystallization mechanism is similar to that of semicrystalline homopolymers involving the formation of macroscopic crystal structures.[15–20]

The nature of nucleation and crystal growth, and how crystallization develops from the melt either from single-phase melt or by destroying existing microphase separated domains was further explored by optical microscopy. Figure 8 shows microscopic images of P55 crystallized at 138°C from the melt under crossed polarizers and at different times during crystallization. The initial melt conditions were the same as the DSC protocol described in the Experimental section. Within the resolution of the microscope, no residual crystallites or other structures were observed in the melt state. This observation indicates that crystallization develops from a single-phase melt structure, in which crystallization dominates the formation of final morphology. Upon reaching the isothermal crystallization temperature, crystal nuclei are observed to form rapidly and grow in size until reaching a constant size as seen in Figure 8(e,f). Some of the crystals impinge against each other but others do not, even after long crystallization times. Because of the limited resolution of the microscope, it is difficult to conclude the nature of nucleation and growth modes from these images. These results suggest the following nucleation and crystal growth possibilities: (1) three-dimensional crystal growth that nucleates with instantaneous (heterogeneous) nucleation or (2) two-dimensional

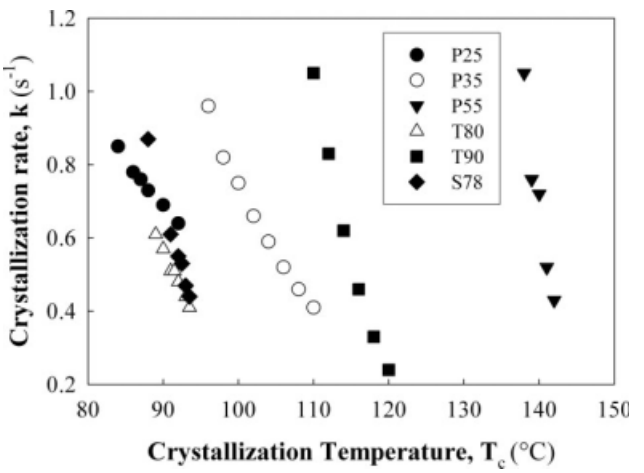

Figure 7 Crystallization rate, k as a function of crystallization temperature obtained from the Kurajica model.

TABLE III
Kinetic Parameters for Isothermal Crystallization of Melt-Blown Samples Obtained by the Kurajica Model

T80								
T_c (°C)	89	90	91	91.5	92	93	93.5	
n	2.98	2.94	2.99	3.02	2.91	3.15	2.97	
k (min^{-1})	0.61	0.57	0.51	0.51	0.48	0.44	0.41	
$t_{1/2}$ (min)	1.45	1.55	1.73	1.74	1.84	2.02	2.16	
T90								
T_c (°C)	110	112	114	116	118	120		
n	2.87	2.99	3.19	3.22	3.32	2.93		
k (min^{-1})	1.05	0.83	0.62	0.46	0.33	0.24		
$t_{1/2}$ (min)	0.84	1.07	1.44	1.94	2.71	3.68		
S78								
T_c (°C)	88	90	92	92.5	93	93.5		
n	2.68	2.63	2.57	2.59	2.57	1.54		
k (min^{-1})	0.87	0.61	0.55	0.53	0.47	0.44		
$t_{1/2}$ (min)	1.00	1.43	1.58	1.64	1.84	1.97		
P25								
T_c (°C)	84	86	87	88	90	92		
n	2.7	2.67	2.65	2.72	2.65	2.87		
k (min^{-1})	0.85	0.78	0.76	0.73	0.69	0.64		
$t_{1/2}$ (min)	1.03	1.12	1.15	1.20	1.26	1.38		
P35								
T_c (°C)	96	98	100	102	104	106	108	110
n	2.95	3.16	3.29	3.27	3.37	3.34	3.41	3.4
k (min^{-1})	0.96	0.82	0.75	0.66	0.59	0.52	0.46	0.41
$t_{1/2}$ (min)	0.92	1.09	1.19	1.35	1.52	1.72	1.95	2.19
P55								
T_c (°C)	138	139	140	141	142			
n	2.77	2.92	3.19	3.19	3.54			
k (min^{-1})	1.05	0.76	0.72	0.52	0.43			
$t_{1/2}$ (min)	0.83	1.16	1.24	1.71	2.10			

crystal growth that nucleates with sporadic (homogeneous) nucleation.[33,34,43] Because crystals appear to be visible around the same time upon reaching the crystallization temperature, three-dimensional crystal growth initiated by heterogeneous nucleation is suggested. Also, compared to the time to reach the ultimate crystallinity, the nucleation time is very short, again indicating heterogeneous nucleation and three-dimensional crystal growth, in agreement with earlier studies on block copolymers.[15–21,44] Similar crystal nucleation and growth were observed for the corresponding hardness grades of ether and ester TPU elastomers (T98 and S95), while crystallites were too small to be observed microscopically for the medium and soft grades of both TPU and PEBA series.

In comparing the crystallization rate for different polymers, it is generally considered better to measure the rate at constant difference in crystallization temperature below the melting temperature, i.e., $\Delta T = T_m - T_c =$ constant. This is illustrated in Figure 9, where k is plotted as a function of the extent of cooling, ΔT. It is clear from Figure 9 that the extent of cooling required to achieve a given crystallization rate follows the order P55 < P35 < P25 for PEBA series, T98 < T90 < T80 for ether TPU series, and S95 < S78 for ester TPU series. Also, at constant ΔT, the crystallization rate, k, decreases with increasing concentration of noncrystallizable component, i.e., soft segment. This means that with increasing amount of crystallizable component, i.e., polymer hard segments, the crystallization of the polymer melt becomes faster, and crystallization onset temperatures shift to higher temperatures, but crystallization onset occurs with a smaller extent of cooling.

The crystallization half-time, $t_{1/2}$, is defined as the time from the onset of the crystallization until the crystallization is half-completed. Based on the Kurajica approach, the crystallization half-time is defined as follows:

$$t_{1/2} = \left(\frac{\ln 2}{k}\right)^{1/n} \tag{5}$$

Typically, the crystallization half-time, shown in Figure 10, is used to represent the overall crystallization rate, which is assumed o be proportional to the inverse of crystallization half-time. Since the crystallization half-time depends on both n and k, comparison of the crystallization rates of different polymers having different n values is not appropriate.[18] However, as seen in Figure 6, the n values determined in this study for all different polymer types and hardness grades do not change significantly and are all around 3. Therefore, the crystallization half-time can be used to compare the overall crystallization rates.

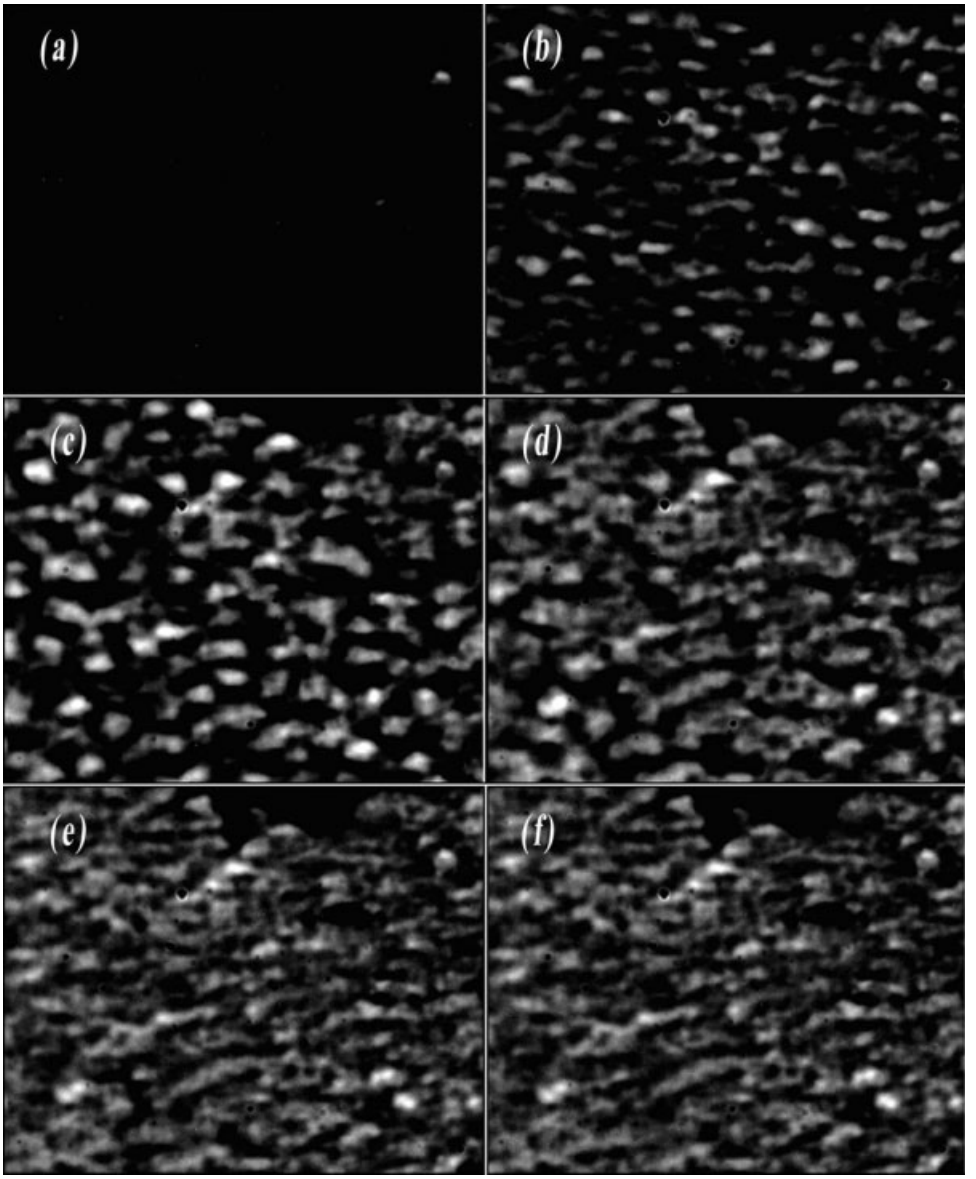

Figure 8 Optical images of the same field of P55 crystallized at $T_c = 138°C$ at crystallization times of (a) 0, (b) 45, (c) 90, (d) 135, (e) 180, and (f) 225 s.

In agreement with the results in Figure 9, the crystallization half-time increases with increasing temperature. The half-time also increases with increasing amount of noncrystallizable soft segment. This means that the crystallization process of the crystallizable hard segment slows down since the noncrystallizable soft segment dilutes the probability for nucleation and crystal growth.[18,30,39,40]

Figure 11 illustrates the dependence of the crystallization half-time on the degree of cooling, which allows comparison of different polymers under similar cooling conditions. In agreement with Figure 10, the degree of cooling required to reach the same crystallization half-time decreases with increasing crystallizable component. Thus, $t_{1/2}$ follows the order of P55 < P35 < P25 for PEBA, T98 < T90 < T80 for ether TPU, and S95 < S78 for ester TPU series. This means that for a given elastomeric copolymer, the increase in the overall crystallization rate is dependent on the relative concentration of the hard and soft segments under similar cooling conditions. This is also evident from the slopes of each curve, where the slope reflects the temperature and composition dependence of the overall crystallization rate.

CONCLUSIONS

Melt-blown webs were produced from the following elastomeric copolymers: (1) BASF Elastollan® Ether TPU series (Shore A): 1180A10, 1190A16, and WY5352D-1; (2) BASF Elastollan® Ester TPU series (Shore A): C78A15 and C95A10; and (3) Arkema

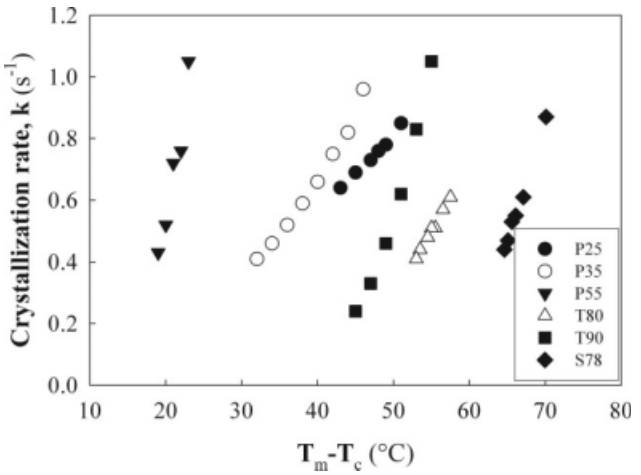

Figure 9 Crystallization rate, k as a function of the degree of cooling.

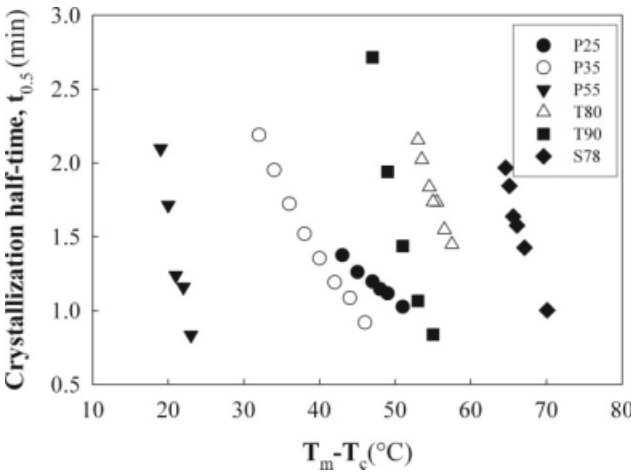

Figure 11 Crystallization half-times of melt-blown webs as a function of the degree of cooling.

Pebax® series (Shore D): 2533, 3533, 5533. The isothermal crystallization kinetics of these melt-blown webs were analyzed through DSC by two different models: (1) the Avrami analysis, which requires transformation of the DSC data from differential to integral form making this traditional method sensitive to errors, and (2) a model proposed by Kurajica et al., which is the derivative of the Avrami equation and could be fitted directly to the untransformed DSC data. The crystallization kinetics parameters, Avrami n and crystallization rate k, derived from both models were comparable and exhibited similar crystallization temperature, polymer type, and hardness dependence. Since the Kurajica model could be directly fitted to the DSC heat flow data, the possible errors involved in the Avrami model were reduced, thereby improving the accuracy of the derived kinetic parameters. The values of the Avrami exponent, n obtained from eq. (3) range between 2.59 and 3.41, suggesting all webs produced from these polymer types have similar nucleation and growth mechanisms, even under different melting and crystallization conditions. These n values of around 3 along with morphological observations indicate that the crystallization mechanism is similar to that of homopolymers involving the formation of macroscopic three-dimensional crystal structures that nucleate and grow with instantaneous nucleation under isothermal conditions. The crystallization rates of all polymer types and hardness grades decreased with increasing crystallization temperatures for lower degree of cooling and concentration of noncrystallizable soft segment. The extent of cooling required to achieve a given crystallization rate followed the order of P55 < P35 < P25 for PEBA series, T98 < T90 < T80 for ether TPU series, and S95 < S78 for ester TPU series. Although among all polymers, P55, the hardest grade of PEBA series, crystallized the fastest at a given extent of cooling, the crystallization rates and half-times of the soft hardness grades for all polymer types, i.e., P25, T80, and S78 were comparable within similar isothermal crystallization temperature ranges. This means that for a given elastomeric copolymer, the overall crystallization rate is dependent on the relative concentration of the hard and soft segments under similar cooling conditions.

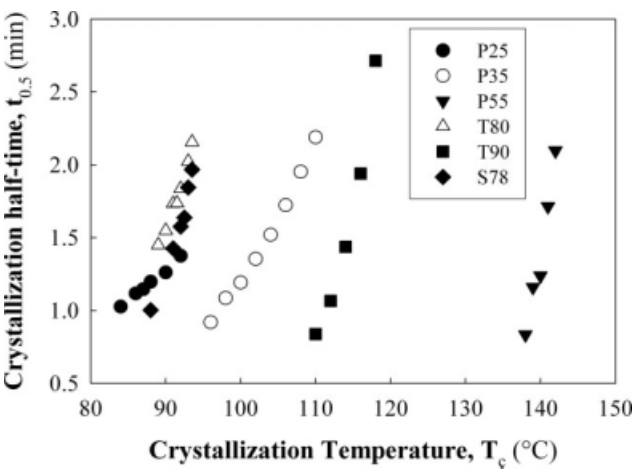

Figure 10 Crystallization half-times of melt-blown webs as a function of T_c.

The authors thank BASF and Arkema for providing the polymer materials, and Birgit Andersen for support during DSC analysis.

References

1. Legge, N. R.; Holden, G.; Schroeder, H. E. Thermoplastic Elastomers: A Comprehensive Review; Hanser: New York, 1987.
2. Konyukhava, E. V.; Buzin, A. I.; Godovsky, Y. K. Thermochim Acta 2002, 391, 271.
3. Alberola, N. J Appl Polym Sci 1988, 36, 787.

4. Nojima, S.; Kato, K.; Yamamoto, S.; Ashida, T. Macromolecules 1992, 25, 2237.
5. Rangarajan, P.; Register, R. A. Macromolecules 1993, 26, 4640.
6. Rangarajan, P.; Register, R. A.; Adamson, D. H.; Fetters, L. J.; Bras, W; Naylor, S.; Ryan, A. J. Macromolecules 1995, 28, 1422.
7. Shiomi, T.; Takeshita, H.; Kawaguchi, H.; Nagai, M.; Takenaka, K.; Miya, M. Macromolecules 2002, 35, 8056.
8. Nojima, S.; Nakano, H.; Ashida, T. Polymer 1993, 34, 4168.
9. Nojima, S.; Nakano, H.; Takahashi, Y.; Ashida, T. Polymer 1994, 35, 3479.
10. Loo, Y.; Register, R. A. Phys Rev Lett 2000, 84, 4120.
11. Chen, H.; Wu, J.; Lin, T.; Lin, J. Macromolecules 2001, 34, 6936.
12. Loo, Y.; Register, R. A. Macromolecules 2001, 34, 8968.
13. Chen, H.; Hsiao, S.; Lin, T.; Yamauchi, K.; Hasegawa, H.; Hashimoto, T. Macromolecules 2001, 34, 671.
14. Loo, Y.; Register, R. A. Macromolecules 2002, 35, 1365.
15. Wegner, G.; Zhu, L.; Lieser, G.; Tu, H. Makromol Chem 1981, 182, 231.
16. Zhu, L.; Wegner, G. Makromol Chem 1981, 182, 3625.
17. Zhu, L.; Wegner, G. Makromol Chem 1981, 182, 3639.
18. Ho, R.; Hseih, P.; Yang, C.; Lin, J. J Polym Sci Part B: Polym Phys 2001, 39, 2469.
19. Seymour, R. W.; Overton, J. R.; Corley, L. S. Macromolecules 1975, 8, 331.
20. Xu, M.; Liu, W. G.; Wang, C. L.; Gao, Z. X.; Yao, K. D. J Appl Polym Sci 1996, 61, 2225.
21. McLean, R. S.; Sauer, B. B. Macromolecules 1997, 30, 8314.
22. Boublil, H.; Okoroafor, E.; Belhoucine, M.; Rault, M.; Atochem, M. G. Polym Eng Sci 1989, 29, 679.
23. Bansal, V.; Davis, M. C.; Ford, T. M.; Massouda, D. F.; Rudisill, E. N.; Samuelson, H. V.; Shin, H.; Weeks, G. P. U.S. Pat. 2003/0171052-A1 (2003).
24. Austin, J. A. U.S. Pat. 6,225,243 (2001).
25. Killian, T. M.; Wisneski, T. J. U.S. Pat. 4,923,742 (1990).
26. Morman, M. T.; Wisneski, T. J. U.S. Pat. 4,741,949 (1988).
27. Makimura, M.; Yamashita, S. U.S. Pat. 4,663,221 (1987).
28. Gessner, S. L.; Newkirk, D. D.; Thomason, M. M.; Reeder, J. O. U.S. Pat. 5,997,989.
29. Begenir, A.; Michielsen, S.; Pourdeyhimi, B. Poly Eng & Sci, to appear.
30. Supaphol, P.; Spruiell, J. E. Polymer 2001, 42, 699.
31. Kurajica, S.; Schmauch, J.; Tkalcec, E. Croat Chem Acta 2002, 75, 693.
32. Zhang, Q.; Yu, M.; Fu, Q. Polym Int 2004, 53, 1941.
33. Mezghani, K.; Phillips, P. J. In Crystallization Kinetics of Polymers; Mark, J. E., Ed. Physical Properties of Polymers Handbook; AIP Press: New York, 1996; Chapter 3.
34. Sharples, A. Polymer Crystallization; Edward Arnold: London, 1966.
35. Mandelkern, L. Crystallization of Polymers; McGraw Hill: New York, 1964.
36. Gu, Q.; Wu, L.; Wu, D.; Shen, D. J Appl Polym Sci 2001, 81, 498.
37. Cassel, R. B.; Sichina, W. J. Better Characterization of Semi-Crystalline Thermoplastics Using Isothermal Crystallization Kinetics, Perkin Elmer Application Note, PETech-47, 2000, http://www.perkinelmer.com (accessed Sept 8, 2008).
38. Ratta, V.; Ayambem, A.; Young, R.; McGrath, J. E.; Wilkes, G. L. Polymer 2000, 41, 8121.
39. Ren, M.; Song, J.; Zhao, Q.; Li, Y.; Chen, Q.; Zhang, H.; Mo, Z. Polym Int 2004, 53, 1658.
40. Liu, M.; Zhao, Q.; Wang, Y.; Zhang, C.; Mo, Z.; Cao, S. Polymer 2003, 44, 2537.
41. Lopez-Manchado, M. A.; Arroyo, M. Polymer 1999, 40, 487.
42. Cho, K.; Li, F.; Choi, J. Polymer 1999, 40, 1719.
43. Ren, M.; Chen, Q.; Song, J.; Zhang, H.; Sun, X.; Mo, Z.; Zhang, H.; Zhang, X.; Jiang, L. J Polym Sci Part B: Polym Phys 2005, 43, 553.
44. Garg, S.; Misra, A. J Polym Sci Polym Lett Ed 1985, 23, 27.